Large elastocaloric effect in Ti–Ni shape memory alloy below austenite finish temperature*

Xiao-Hua Luo(罗小华)[1], Wei-Jun Ren(任卫军)[1,†], Wei Jin(金伟)[2], and Zhi-Dong Zhang(张志东)[1]

[1] *Shenyang National Laboratory for Materials Science, Institute of Metal Research, Chinese Academy of Sciences, Shenyang* 110016, *China*
[2] *Institute of Metal Research, Chinese Academy of Sciences, Shenyang* 110016, *China*

(Received 24 October 2016; revised manuscript received 10 December 2016; published online 13 February 2017)

Solid refrigeration technology based on the elastocaloric effect has a great potential alternative to the conventional vapor compression cooling. Here we report the large elastocaloric effect in Ti–Ni (50 at%) shape memory alloy below its austenite finish temperature A_f under different strain. Both Maxwell's and Clausius–Clapeyron equations are used to estimate the entropy change. The strain-induced entropy change increases with raising the strain and gets a maximum value at a few kelvins below A_f. The maximum entropy changes ΔS_{max} are -20.44 and -53.70 J/kg·K, respectively for 1% and 2% strain changes. Large entropy change may be obtained down to 20 K below A_f. The temperature of the maximum entropy change remains unchanged before the plastic deformation appears but moves towards low temperature when the plastic deformation happens.

Keywords: elastocaloric effect, martensitic transformation, shape memory alloys

PACS: 65.40.De, 46.25.Hf, 62.20.fg **DOI:** 10.1088/1674-1056/26/3/036501

1. Introduction

Solid refrigeration technologies based on magnetocaloric effect, electrocaloric effect, and elastocaloric effect have been widely investigated in recent years because of a potential alternative to the conventional vapor compression cooling.[1–16] The elastocaloric effect is defined as the isothermal entropy change or the adiabatic temperature change under a mechanical stress, which is directly related to the phenomenon of reversible solid-to-solid martensitic phase transformation.[17,18] Even though the elastocaloric effect was reported as early as in the beginning of the 19th century, it has drawn much attention only since Bonnot *et al*. reported the elastocaloric effect in Cu–Zn–Al single crystal in 2008.[15,17] Since then, the elastocaloric effects of series of shape memory alloys such as Ti–Ni–(Cu),[18–22] Fe–Pd,[23,24] Ni–Mn-based,[25–27] and Ni–Fe-based[16,22,28] shape memory alloys have been reported. Martensitic phase transformation is induced by applying a uniaxial stress and the reverse transformation takes place by releasing the stress. Above the austenite finish temperature A_f, strain can be recovered entirely after unloading, which is known as superelastic effect. The transformation strain contributes essentially to the isothermal entropy change or the adiabatic temperature change.[23] Therefore, up to now, the investigation of the elastocaloric effect predominantly focuses on the temperature range above A_f. In the case of temperature below A_f, due to the coexistence of parent phase and martensitic phase, the stress-induced martensitic transformation and detwinning/twinning martensites develop simultaneously upon loading, which is much more complex than the situation of the temperature above A_f.[29] So investigating the elastocaloric effect below A_f is indispensable and meaningful to a comprehensive understanding of the elastocaloric effect of shape memory alloys. In this work, we study the elastocaloric effect in Ti–Ni (50 at%) shape memory alloy below A_f under different strains.

2. Experiment

The samples were cut from a long Ti–Ni (50 at%) bar and machined with cylindrical heads threaded and the bodies were also cylindrical with 10 mm in diameter and 60 mm in length. The samples were annealed at 973 K for 3 hours, and then quenched into water. The differential scanning calorimetry (DSC) thermograms were recorded using DSC Q20 V24.10 build 122 Instrument, at the rate of 10 K/min.

Tensile experiments were carried out by Instron 5982 tensile testing machine with temperature ranging from 323 K to 363 K. The experimental protocol comprised the following steps. First, the sample was loaded at a rate of 3.6 mm/min to maximum strain and unloaded at a rate of 1.5 mm/min at constant experimental temperature. The maximum strain was set as 1%, 2%, and 6%, respectively. Second, the sample was heated to 473 K and kept for 30 minutes, then cooled to room temperature.

*Project supported by the National Natural Science Foundation of China (Grant Nos. 51671192 and 51531008) and the Chinese Academy of Sciences (Grant No. KJZD-EW-M05).

†Corresponding author. E-mail: wjren@lmr.ac.cn

© 2017 Chinese Physical Society and IOP Publishing Ltd

3. Results and discussion

Figure 1 shows DSC curves of heating and cooling processes at a rate of 10 K/min. The martensite start temperature M_s, austenite start temperature A_s, and austenite finish temperature A_f, were determined to be 342 K, 303 K, and 361 K respectively. The total entropy change in martensitic transformation can be determined by

$$\Delta S^{\text{tol}} = \frac{\Delta H}{T_0}, \tag{1}$$

where ΔH is the transformation enthalpy change and T_0 is the equilibrium temperature defined as $(M_s + A_f)/2$.[30] From the DSC measurement of our sample, T_0 is 351.5 K and ΔH is -11190 J/kg, ΔS^{tol} was calculated to be -31.83 J/kg·K.

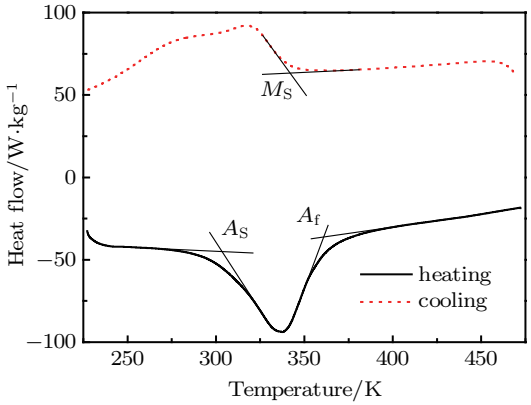


Fig. 1. (color online) DSC curve at the rate of 10 K/min.

Figure 2(a) displays the stress–strain curves obtained at different temperatures when the maximum strain is 1%. The residual strain after unloading decreases with increasing temperature. When temperature is above 359 K, the strain recovers almost entirely, indicating that the superelasticity and the stress-induced martensitic transformation occur in consistence with the DSC results. The residual strain is derived from the lattice invariant strain induced by detwinning/twinning of martensite variant and it can be recovered by heating up to 473 K. As a result, the length of the sample remains almost unchanged after this experiment. The stress–strain curves for the maximum strain of 2% are presented in Fig. 2(b). Similar to that of the maximum strain of 1%, the residual strain after unloading decreases with increasing temperature above 331 K and it is recoverable by heating up to 473 K. Thus, it can be attributed to the lattice invariant strain. When the maximum strain is 6%, the stress–strain curves are shown in Fig. 2(c). In this case, the residual strain after unloading of two measurements cannot recover entirely by heating up to 473 K and remains about 1%, which indicates the plastic deformation. This means the coexistence of three deformation modes in these processes, that is, the unrecoverable plastic deformation caused by the movement of dislocations, the detwinning/twinning martensites deformation that is recoverable when heating, and the stress-induced martensites deformation that is spontaneous recovering after unloading. Below 351 K, loading stress–strain curves display S-like shape. It disappears above 355 K because of the increment of the critical stress.

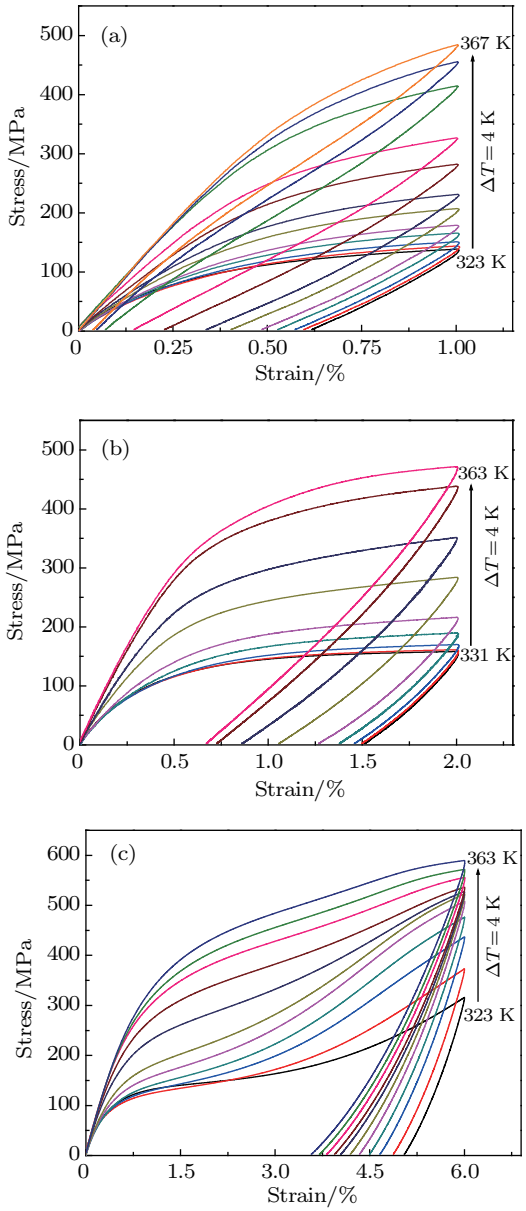


Fig. 2. (color online) Stress–strain curves obtained at selected temperature. The maximum strain is 1% (a), 2% (b) and 6% (c). The temperature interval is 4 K.

For a smooth stress–strain curve, it is not easy to define the critical stress that is required to induce martensitic transformation. An offset point $\sigma_{0.1}$ is commonly arbitrarily set at 0.1% plastic strain.[31] The definition method was illustrated in Fig. 3(a). This method is widely used in engineering to define the offset yield strength $\sigma_{0.2}$ of high strength steel and aluminum alloy. The temperature dependences of $\sigma_{0.1}$ with the maximum strain of 1%, 2%, and 6% are shown in Fig. 3(a). For every case of the maximum strain of 1%, 2%, and 6%,

the critical stress changes gently below 340 K. However, it increases almost linearly above 340 K, until temperature is close to A_f. Our result is consistent with the temperature dependence of the critical stress of Ti–Ni alloy reported by Melton *et al.*[31] The critical stress curve for the maximum strain of 1% is almost parallel to that of 2%, but not parallel to that of 6%. It indicates that the detwinning/twinning martensites do not have much contribution to the critical stress slope $\frac{d\sigma}{dT}$, but the plastic deformation has distinct effect on $\frac{d\sigma}{dT}$. The temperature dependences of $\frac{d\sigma}{dT}$ for the maximum strain of 1%, 2%, and 6% are shown in Fig. 3(b).

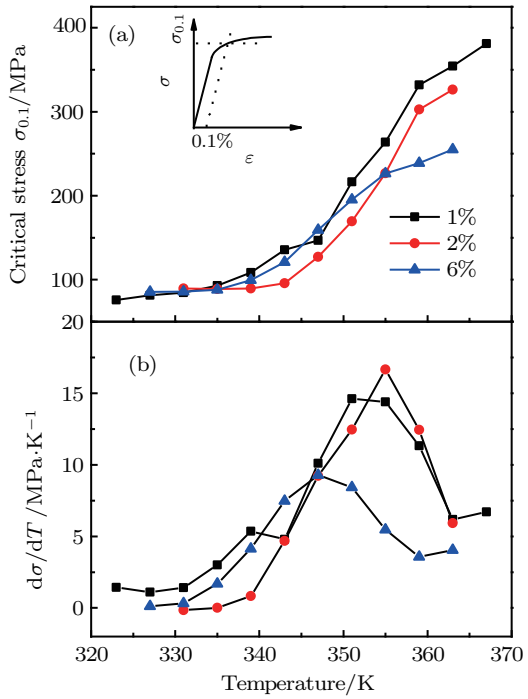


Fig. 3. (color online) Temperature dependences of (a) critical stress $\sigma_{0.1}$ and (b) critical stress slope $\frac{d\sigma}{dT}$ for 1%, 2%, and 6% strain change. The scheme plot in (a) illustrates the method to define $\sigma_{0.1}$.

For the elastocaloric effect, the isothermal entropy change ΔS and the adiabatic temperature change ΔT induced by strain ε may be determined by using[5]

$$\Delta S(0 \to \varepsilon) = -\int_0^{\varepsilon} \left(\frac{\partial \sigma}{\partial T}\right)_{\varepsilon} d\varepsilon, \tag{2}$$

$$\Delta T = -\frac{T}{C_p}\Delta S, \tag{3}$$

where C_p is the specific heat. According to the Clausius–Clapeyron relationship, the entropy change of the transformation can also be calculated by[5]

$$\Delta S = -\frac{d\sigma}{dT}\varepsilon_t, \tag{4}$$

where $\frac{d\sigma}{dT}$ is the Clausius–Clapeyron slope, and ε_t is the transformation strain.

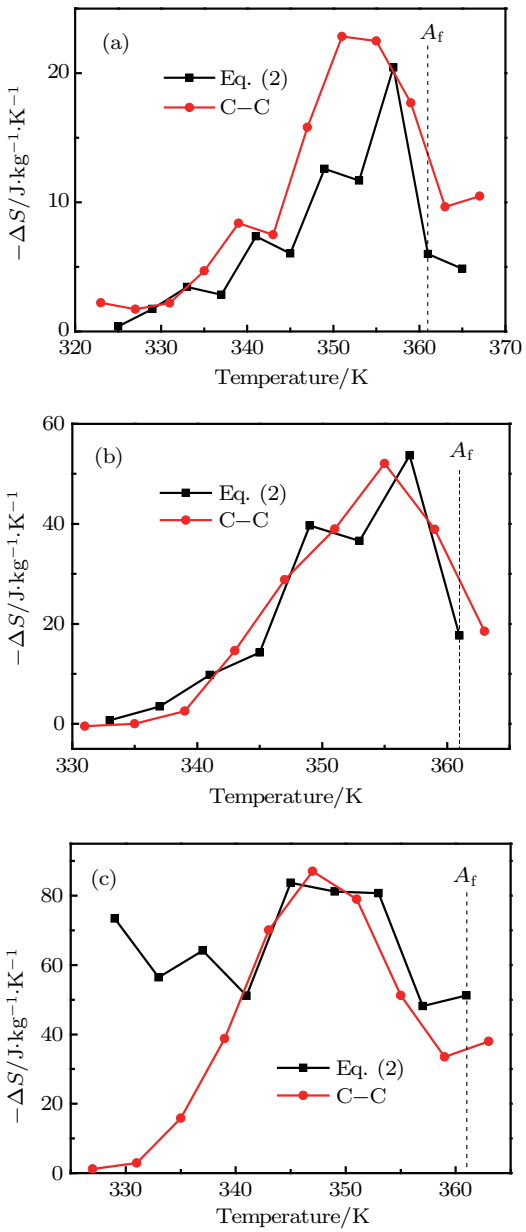


Fig. 4. (color online) Strain-induced entropy changes for the strain changes of 1% (a), 2% (b), and 6% (c). The squares are estimated by Eq. (2) and the circles are estimated by the Clausius–Clapeyron equation.

Using Eq. (2) and the density ρ of 6.4×10^3 kg/m^2, we calculated the strain-induced entropy changes of the studied Ti–Ni alloy for the maximum strain changes of 1%, 2%, and 6%, respectively, which are displayed in Fig. 4. It is seen that large entropy changes are obtained in all of our study down to 20 K below A_f. When the maximum strain changes are 1% and 2%, the trends of the entropy change with temperature are similar to that of $\frac{d\sigma}{dT}$. With increasing temperature, the entropy change increases and reaches the maximum at the temperature of 357 K, a few kelvins below A_f, then decreases sharply. The maximum entropy changes ΔS_{max} are -20.44 and -53.70 J/kg·K, respectively for 1% and 2% strain change. The temperature dependence of the entropy change ΔS for the strain change of 6% is very different from those obtained for

the maximum strain change of 1% and 2%, and the entropy changes ΔS are very large. The ΔS at almost all the temperatures in this study are larger than -50 J/kg·K. The maximum value is -83.74 J/kg·K at 345 K. The strain-induced entropy changes estimated by the Clausius–Clapeyron equation are also displayed in Fig. 4. For simplicity, we take the total strain 1%, 2%, and 6% as the transformation strain ε_t. The results match well with the values obtained from the Clausius–Clapeyron equation, except for the strain change of 6%. When the maximum strain changes are 1% and 2%, the plastic deformation does not occur. Since the temperature dependences of two critical stresses are almost parallel, the critical stress slopes are almost the same. As a consequence, the trends of the entropy change of the two cases are similar. When the maximum strain change is 6%, their reversible plastic deformation takes place, which results in the change of the critical stress slope, and makes the peak of the critical stress slope move towards relatively low temperature. Therefore, the temperature of the maximum entropy change for 6% strain change is lower than those for 1% and 2% strain changes.

The temperature dependence of the elastocaloric effect below A_f is quite different from that above A_f. As we have known, as in Cu–Zn–Al crystal, when temperature is above A_f, the critical stress inducing the martensitic transformation increases linearly with increasing temperature, so $\frac{d\sigma}{dT}$ is almost constant. Thus the variation of the strain-induced entropy change with temperature is small above A_f in Cu–Zn–Al crystal. However, when temperature is below A_f, because of the existence of the detwinning/twinning martensites deformation, $\frac{d\sigma}{dT}$ changes with temperature. It is shown by our work that the slope of the critical stress increases with increasing temperature and reaches a maximum at the temperature a little below A_f. Thus, the strain-induced entropy change has a large variation with temperature.

4. Conclusions

In summary, the elastocaloric properties of Ti–Ni (50 at%) alloy have been experimentally studied by the stress–strain curves for 1%, 2%, and 6% strain changes around A_f. Large strain-induced entropy change was obtained down to 20 K below A_f. The maximum value appears at a few kelvins below A_f. Before the plastic deformation happens, the maximum entropy change increases with rising strain, while the temperature of the maximum entropy change remains unchanged. When the plastic deformation occurs, the temperature of the maximum entropy change lowers.

References

[1] Pecharsky V K and Gschneidner J K A 1997 *Phys. Rev. Lett.* **78** 4494
[2] Gschneidner J K A, Pecharsky V K and TsokolA O 2005 *Rep. Prog. Phys.* **68** 1479
[3] Shen J, Li Y X, Sun J R and Shen B G 2009 *Chin. Phys. B* **18** 2058
[4] Manosa L, Gonzalez-Alonso D, Planes A, Bonnot E, Barrio M, Tamarit J L, Aksoy S and Acet M 2010 *Nat. Mater.* **9** 478
[5] Hu F X, Shen B G and Sun J R 2013 *Chin. Phys. B* **22** 037505
[6] Shen B G, Hu F X, Dong Q Y and Sun J R 2013 *Chin. Phys. B* **22** 017502
[7] Tegus O, Bao L H and Song L 2013 *Chin. Phys. B* **22** 037506
[8] Wang D H, Han Z D, Xuan H C, Ma S C, Chen S Y, Zhang C L and Du Y W 2013 *Chin. Phys. B* **22** 077506
[9] Mischenko A S, Zhang Q, Scott J F, Whatmore R W and Mathur N D 2006 *Science* **311** 1270
[10] Neese B, Chu B J, Lu S G, Wang Y, Furman E and Zhang Q M 2008 *Science* **321** 821
[11] Qiu J H, Ding J N, Yuan N Y and Wang X Q 2012 *Chin. Phys. B* **21** 097701
[12] Qiu J H, Ding J N, Yuan N Y and Wang X Q 2013 *Chin. Phys. B* **22** 017701
[13] Fähler S, Röessler U K, Kastner O, Eckert J, Eggeler G, Emmerich H, Entel P, Mueller S, Quandt E and Albe K 2012 *Adv. Eng. Mater.* **14** 10
[14] Manosa L, Planes A and Acet M 2013 *J. Mater. Chem. A* **1** 4925
[15] Moya X, Kar-Narayan S and Mathur N D 2014 *Nat. Mater.* **13** 439
[16] Xu Y, Lu B F, Sun W, Yan A R and Liu J 2015 *Appl. Phys. Lett.* **106** 201903
[17] Bonnot E, Romero R, Manosa L, Vives E and Planes A 2008 *Phys. Rev. Lett.* **100** 125901
[18] Cui J, Wu Y, Muehlbauer J, Wang Y H, Radermacher R, Fackler S, Wuttig M and Takeuchi I 2012 *Appl. Phys. Lett.* **101** 073904
[19] Bechtold C, Chluba C, De Miranda R L and Quandt E 2012 *Appl. Phys. Lett.* **101** 091903
[20] Ossmer H, Lambrecht F, Gueltig M, Chluba C, Quandt E and Kohl M 2014 *Acta Mater.* **81** 9
[21] Tušek J, Engelbrecht K, Mikkelsen L P and Pryds N 2015 *J. Appl. Phys.* **117** 124901
[22] Pataky G J, Ertekin E and Sehitoglu H 2015 *Acta Mater.* **96** 420
[23] Xiao F, Fukuda T and Kakeshita T 2013 *Appl. Phys. Lett.* **102** 161914
[24] Xiao F, Fukuda T, Kakeshita T and Jin X 2015 *Acta Mater.* **87** 8
[25] Castillo-Villa P O, Manosa L, Planes A, Soto-Parra D E, Sanchez-Llamazares J L, Flores-Zuniga H and Frontera C 2013 *J. Appl. Phys.* **113** 053506
[26] Lu B F, Xiao F, Yan A R and Liu J 2014 *Appl. Phys. Lett.* **105** 161905
[27] Millan-Solsona R, Stern-Taulats E, Vives E, Planes A, Sharma J, Nayak A K, Suresh K G and Manosa L 2014 *Appl. Phys. Lett.* **105** 241901
[28] Xiao F, Jin M J, Liu J and Jin X J 2015 *Acta Mater.* **96** 292
[29] Otsuka K and Ren X 2005 *Prog. Mater. Sci.* **50** 511
[30] Tong H C and Wayman C M 1974 *Acta Metall.* **22** 887
[31] Melton K N and Mercier O 1981 *Acta Metall.* **29** 393